Phys. Status Solidi A **214,** No. 3, 1600617 (2017) / **DOI** 10.1002/pssa.201600617

physica status solidi a
www.pss-a.com
applications and materials science

Neutral beam etching for device isolation in AlGaN/GaN HEMTs

Fuyumi Hemmi*[,1], Cedric Thomas[2], Yi-Chun Lai[3], Akio Higo[3], Alex Guo[4], Shireen Warnock[4], Jesús A. del Alamo[4], Seiji Samukawa[2,3], Taiichi Otsuji[1], and Tetsuya Suemitsu[1]

[1] Research Institute of Electrical Communication, Tohoku University, 2-1-1 Katahira, Aoba-ku, 980-8577 Sendai, Japan
[2] Institute of Fluid Science, Tohoku University, 2-1-1 Katahira, Aoba-ku, 980-8577 Sendai, Japan
[3] Advanced Institute of Materials Research, Tohoku University, 2-1-1 Katahira, Aoba-ku, 980-8577 Sendai, Japan
[4] Microsystems Technology Laboratories, Massachusetts Institute of Technology, 77 Massachusetts Avenue, Cambridge, MA 02139, USA

Received 14 August 2016, revised 26 October 2016, accepted 14 November 2016
Published online 28 November 2016

Keywords breakdown voltage, GaN, high electron mobility transistor, leakage current, neutral beam etching, plasma damage

* Corresponding author: e-mail hemmi@riec.tohoku.ac.jp, Phone: +81 22 217 6108, Fax: +81 22 217 6108

In this article, we report a suppression of leakage current and an improvement of isolation breakdown voltage on GaN-based high electron mobility transistors (HEMTs) by means of neutral beam (NB) etching. The plasma damage during dry etching process is one of the key reasons for an isolation leakage current, gate leakage current, and current collapse in GaN HEMTs. Since NB etching is virtually free from electrical charges and has few UV photons, it is possible to reduce plasma damage on an etched surface and improve device characteristics. In this work, we introduced NB etching to the device isolation process of GaN HEMTs and characterized isolation leakage currents at DC and step-stress bias conditions. We also measured the breakdown voltages on two-terminal test element arrays. We compared the characteristics with samples etched by conventional plasma-like beam (PB) etching. Our results suggest that NB etching reduces the leakage current through the etched surface of the mesa isolation, which results in superior breakdown voltages.

1 Introduction GaN-based high electron mobility transistors (HEMTs) are promising for both power and high-frequency applications [1–5]. These applications include the wireless communication systems in microwave and millimetre-wave bands, as well as the high-voltage switching devices used in, for example, automotive vehicles [6, 7]. Since many of these applications require high levels of device reliability, any process damage induced in GaN, and related materials are major concerns. On the other hand, GaN-based materials are hard materials that are difficult to etch by wet chemical approaches. Thus these materials are usually etched by dry etching such as Inductively Coupled Plasma (ICP) etching and Reactive Ion Etching (RIE). However, such a plasma etching may cause plasma damages at the etched surface. In addition, UV photons included in the plasma discharge can produce deep traps in semiconductors [8–11]. The carrier trapping phenomena causes a leakage current path through the damaged surface, resulting in decreased breakdown voltage. These UV photons are difficult to eliminate while using conventional plasma etching.

In this study, we introduced neutral beam (NB) etching [8] to the device isolation process of GaN-based HEMTs. Figure 1(a) shows the NB etching system. This equipment consists of two chambers; a plasma chamber and an etching chamber. A carbon electrode with an aperture array is set between the two chambers as a bottom electrode. In the plasma chamber, inductively coupled plasma is produced from Cl_2 gas by a high frequency electromagnetic field with an RF power of 800 W. When plasma ions pass through the carbon electrode, ion particles are neutralized and UV photons are eliminated [12]. As a result, the NB realizes damage-free etching. The neutralization of the plasma beam can be controlled by changing the aspect ratio of the carbon aperture shown in Fig. 1(b).

We measured the isolation leakage currents, the evolution of the leakage current under step stress [13–15], and the isolation breakdown voltages in both samples produced by NB etching versus conventional plasma-like beam (PB) etching. The PB etching was carried out using the same equipment as the NB etching, but with the bottom

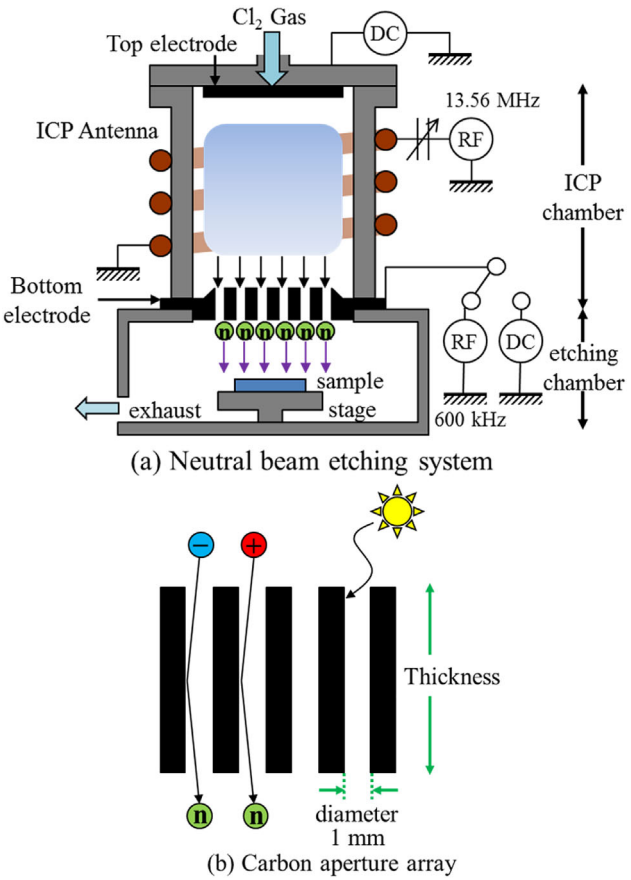

Figure 1 (a) Schematic of neutral beam etching system and (b) enlarged figure of carbon aperture array. The aspect ratio is defined as the ratio of carbon thickness and diameter.

electrode replaced by carbon aperture with lower aspect ratio, so that charged particles and UV photons can enter into the etching chamber. We also compared samples with and without a passivation coating (SiN) for both NB and PB etching to examine the effects on isolation leakage.

2 Sample fabrication process The epitaxial structure consists of a 15.6-nm-thick AlGaN barrier layer, a 2000-nm-thick GaN channel layer and a buffer layer grown on a *c*-plane sapphire substrate, as shown in Fig. 2(a). The mobility and concentration of the two-dimensional electron gas are 1531 $cm^2/V\,s$ and $9.0 \times 10^{12}\,cm^{-2}$ at room temperature, respectively.

The fabrication of test samples followed our standard GaN HEMT process [16–18]. We started with the ohmic metallization, followed by mesa isolation, and then ohmic annealing with a SiO_2 protection coating was performed. The formation of ohmic electrodes was done by Ti/Al/Ni/Au (20/120/20/70 nm) lift-off. Then the mesa isolation was carried out by either NB or PB. The NB and PB were produced with the same equipment by choosing different aspect ratio of carbon aperture (thickness over diameter in Fig. 1(b)) of 10 for NB and 2 for PB with an aperture diameter of 1 mm. The NB and PB were carried

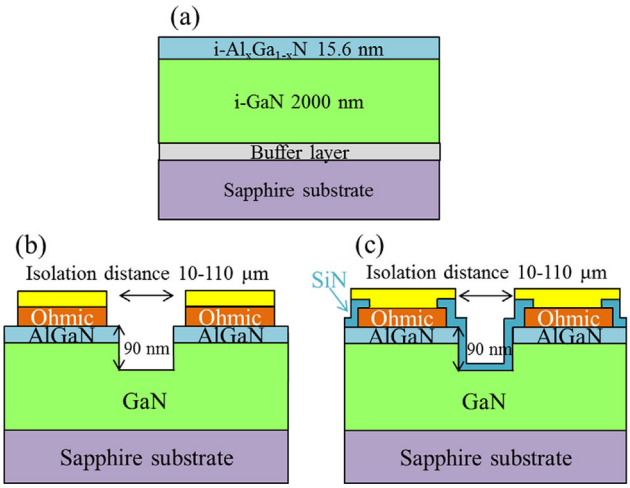

Figure 2 Cross sectional view of (a) epitaxial layer structure, (b) NB/PB etching sample without passivation, and (c) NB/PB etching sample with passivation.

out with Cl_2 gas at 0.09 Pa and an RF power of 800 W. The etching rate is shown in Table 1. The etching conditions were calibrated to achieve an etching depth of 90 nm. The RMS (Root Mean Square) roughness was 0.427 nm for a NB sample and 2.226 nm for a PB sample analyzed with atomic force microscope (AFM). After isolation, a 300-nm-thick SiO_2 film was deposited by plasma-enhanced chemical vapor deposition (PECVD) at 350 °C to protect the device surface from high temperature annealing. Then, ohmic annealing was carried out at 780 °C for 2 min in N_2 ambient. Subsequently, the SiO_2 film was removed by buffered HF solution. To consider the effect of the passivation coating, four types of samples were prepared; NB samples with passivation (NB-P), NB samples without passivation (NB), PB samples with passivation (PB-P), and PB samples without passivation (PB). For NB-P and PB-P types, samples were passivated with a 200-nm-thick SiN film by PECVD at 250 °C, then the SiN layer on the ohmic electrodes were removed by reactive ion etching (RIE) with SF_6 to open the contact holes. Finally, Ti/Ni/Au (20/20/350 nm) pad electrodes were evaporated and lifted off for all types of samples.

The cross sectional views of the four types of samples are shown in Fig. 2(b) and (c). Two-terminal devices with isolation distances from 10 to 110 μm were prepared for each type of sample.

Table 1 Etching parameters for PB and NB.

beam	aspect ratio	etching rate (AlGaN)	etching rate (GaN)
NB	10	5 nm/min	10 nm/min
PB	2	7.5 nm/min	15 nm/min

3 Results and discussion

3.1 Leakage current measurements In the leakage current measurement, we measured I–V characteristics with voltage sweep of 0–40 V and extracted the current values under 4 V. Figure 3 shows the isolation leakage current at an applied voltage of 4 V on (a) a linear scale and (b) a logarithmic scale as a function of the isolation distance from 10 to 110 μm. The results of the samples with passivation coating clearly indicate that NB-P samples exhibit lower leakage current than that in PB-P samples, suggesting that the NB etching effectively reduces plasma damages on the etched surface.

On the other hand, the samples without passivation shows significantly lower levels of leakage current than those with passivation coating. Since the current conduction through the passivation film is considered as one of the possibility, the conductivity of SiN film was characterized. However, the conductivity of SiN was negligible (less than pA/mm). Hence, the conduction through the SiN film is ruled out. Thus the excess leakage current is most likely because PECVD of the passivation film causes plasma damage on the samples with passivation as mentioned in Section 2. However, Fig. 3(b) shows that the leakage current of the samples without passivation was so unstable that it was difficult to obtain a reliable and reproducible comparison between NB and PB samples. Therefore, the passivation film is indispensable and hence a plasma-free effective passivation process should be developed to eliminate the plasma damages from devices.

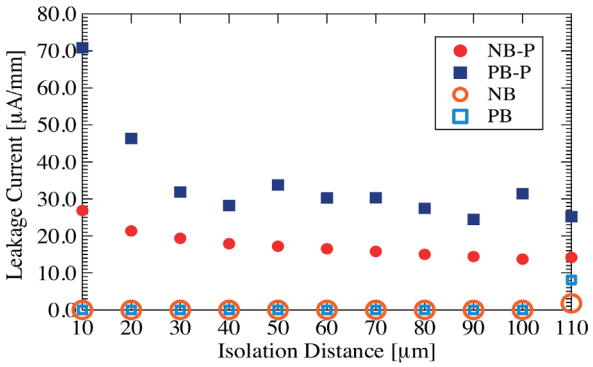

(a) Linear plot

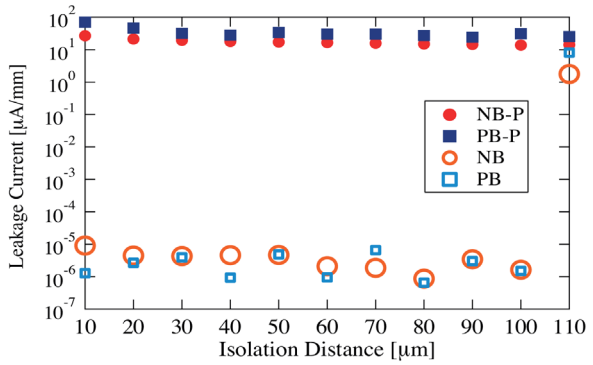

(b) Semilogarithmic plot

Figure 3 Leakage current on (a) linear scale and (b) logarithmic scale measured on two-terminal devices with different isolation distances. Applied voltage is 4 V. Samples with passivation (NB-P and PB-P) and without passivation (NB and PB) are plotted.

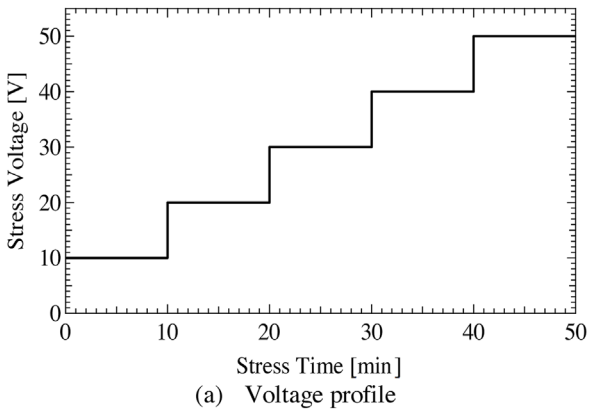

(a) Voltage profile

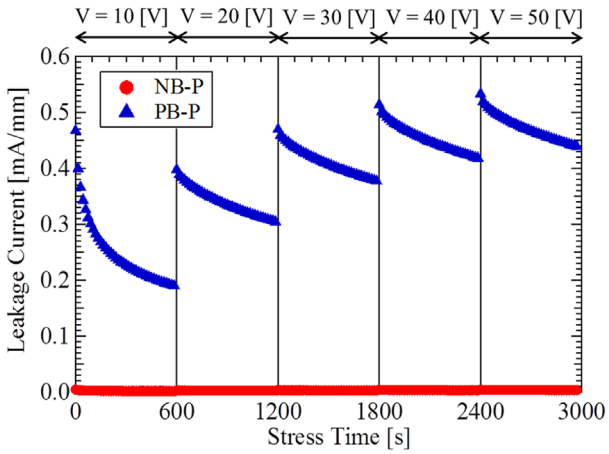

(b) Linear plot

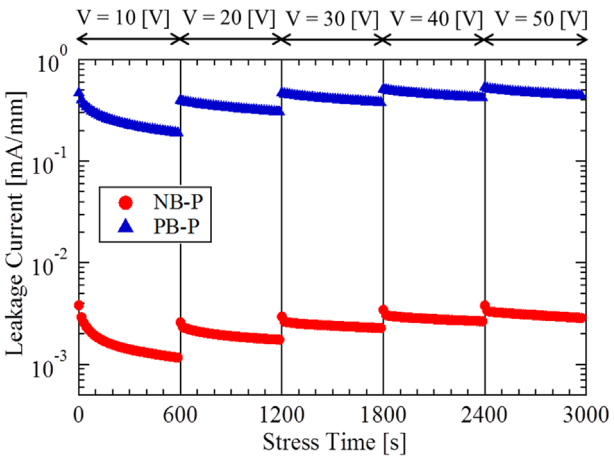

(c) Semilogarithmic plot

Figure 4 Change in leakage current under step-stress tests. (a) Voltage profile and leakage current on (b) a linear scale and (c) a logarithmic scale as a function of the stress time.

3.2 Step stress measurements The step-stress measurements were carried out as follows: the stress voltage was increased from 10 to 50 V in 10 V steps with a stress time of 10 min for each step as shown in Fig. 4(a). The transient response of the leakage current gives us information about deep trap levels playing a role in the isolation leakage current [13–15]. Since Fig. 3 indicates that the leakage current significantly decreases with increasing isolation distance from 10 to 40 μm, additional sources of the leakage current in this range of the distance still exist. Thus we carried out the step-stress measurements using devices with a longer isolation distance (70 μm).

Figure 4 shows the leakage current on (b) a linear scale and (c) a logarithmic scale as a function of the stress time. Focusing on the samples with a passivation film, NB-P samples exhibit 10 times lower leakage current than in PB-P samples, as expected from the results shown in Fig. 3. In PB-P samples, larger amounts of current decrease are observed at each voltage step than in NB samples. Such current decreases can be considered to be the result of filling charges in deep traps and therefore, NB samples have fewer deep traps than PB samples. These results further confirm the advantages of NB etching over conventional plasma etching.

3.3 Breakdown voltage measurements To carry out a systematic analysis of the isolation breakdown voltage, we defined the soft breakdown voltage (SBV) as the voltage at which the leakage current reaches 1 mA/mm [19]. SBV was characterized for NB-P and PB-P samples. In addition, NB-P samples with an isolation etching depth of 30 nm (NB-P-30 nm) were also characterized. The measurement limit of our equipment (Keysight B2912A) is 210 V. Figure 5 shows the SBV as a function of isolation distance. The average value of SBV is 25.6 V for PB-P sample and 45.7 V for NB-P-30 nm. Since NB-P samples exhibited one order of magnitude less leakage current than 1 mA/mm, these devices did not reach SBV within the measurement limit. These results suggest that NB-P samples have over 10 times higher SBVs than those for the PB-P samples. Also, the effect of etching depth is clearly indicated by comparing NB-P and NB-P-30 nm.

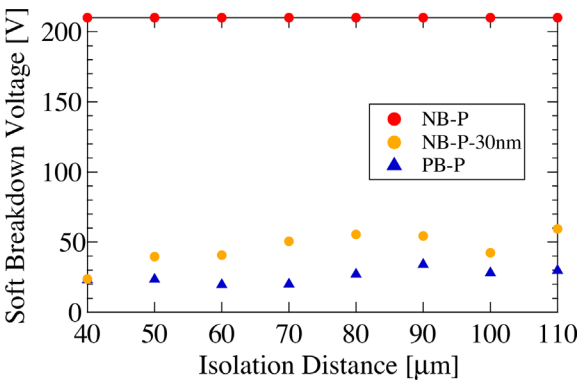

Figure 5 Soft breakdown voltages (SBVs) in passivated two-terminal devices etched by NB and PB. Results on NB-etched samples with a depth of 30 nm are also shown. SBVs of NB-P samples are over the measurement limit (210 V).

We also measured the hard (catastrophic) breakdown voltage of PB-P and NB-P-30 nm by applying a voltage sweep up to 1500 V, or until the device was burned out, for the devices with isolation distances from 50 to 110 μm. NB-P-30 nm samples exhibited hard breakdown voltages of over 800 V while PB-P samples exhibited hard breakdown voltages from 600 to 700 V. Therefore, the advantage of NB-P-30 nm over PB-P observed in SBV is also manifested on the hard breakdown voltage. As a consequence NB-P samples are expected to outperform these samples in hard breakdown characteristics.

4 Conclusions We experimentally confirmed that the neutral beam etching helps suppress the isolation leakage current in AlGaN/GaN HEMTs. As a result, the neutral beam etching has an impact to increase the isolation breakdown voltage by one order of magnitude in comparison to the conventional plasma etching. Based on these results and step stress characteristics, we believe that NB etching is effective to reduce plasma-induced damages on the etched surface of GaN. Therefore, the neutral beam etching is a promising tool in the fabrication of GaN-based power devices.

Acknowledgements This work was supported by the JSPS KAKENHI grant number JP15K13963, JP16H04341, Japan, and the Tohoku University-MIT collaboration initiative program by RIEC, Tohoku University, Japan. The device fabrication process was carried out at the Laboratory for Nanoelectronics and Spintronics at RIEC, Tohoku University, Japan.

References

[1] K. Shiohara, D. Regan, A. Corrion, D. Brown, S. Burnham, P. J. Willadsen, I. Alvarado-Rodriguez, M. Cunningham, C. Butler, A. Schmitz, S. Kim, B. Holden, D. Chang, V. Lee, A. Ohoka, P. M. Asbeck, and M. Micovic, IEDM Tech. Dig. 453–456 (2011).
[2] Y. Yue, Z. Hu, J. Guo, B. Sensale-Rodriguez, G. Li, R. Wang, F. Faria, T. Fang, B. Song, X. Gao, S. Guo, T. Kosel, G. Snider, P. Fay, D. Jena, and H. Xing, IEEE Electron Device Lett. **33**, 988 (2012).
[3] R. Wang, G. Li, G. Karbasian, J. Guo, F. Faria, Z. Hu, Y. Yue, J. Verma, O. Laboutin, Y. Cao, W. Johnson, G. Snider, P. Fay, D. Jena, and H. Xing, Appl. Phys. Express **6**, 016503 (2013).
[4] S. Arulkumaran, G. I. Ng, S. Vicknesh, H. Wang, K. S. Ang, C. M. Kumar, K. L. Teo, and K. Ranjan, Appl. Phys. Express **6**, 016501 (2013).
[5] T. Suemitsu, K. Kobayashi, S. Hatakeyama, N. Yasukawa, T. Yoshida, T. Otsuji, D. Piedra, and T. Palacios, Jpn. J. Appl. Phys. **55**, 01AD02 (2016).
[6] T. Kachi, Jpn. J. Appl. Phys. **53**, 100210 (2014).
[7] G. Meneghesso, M. Meneghini, and E. Zanoni, Jpn. J. Appl. Phys. **53**, 100211 (2014).
[8] S. Samukawa, Jpn. J. Appl. Phys. **45**, 2395–2407 (2006).
[9] R. Kawakami, T. Inaoka, S. Minamoto, and Y. Kikuhara, Thin Solid Films. **516**, 3478–3481 (2008).

[10] R. Kawakami, T. Inaoka, K. Tominaga, A. Kuwahara, and T. Mukai, Jpn. J. Appl. Phys. **47**, 6863–6866 (2008).
[11] M. Minami, S. Tomiya, K. Ishikawa, R. Matsumoto, S. Chen, M. Fukasawa, F. Uesawa, M. Sekine, M. Hori, and T. Tatsumi, Jpn. J. Appl. Phys. **50**, 08JE03 (2011).
[12] S. Samukawa, Y. Ishikawa, K. Okumura, Y. Sato, K. Tohji, and T. Ishida, J. Phys. D: Appl. Phys. **41**, 024006 (2008).
[13] J. Joh and J. A. del Alamo, IEDM Tech. Dig. 415–418 (2006).
[14] G. Meneghesso, G. Verzellesi, F. Danesin, F. Rampazzo, F. Zanon, A. Tazzoli, M. Meneghini, and E. Zanoni, IEEE Trans. Device Mater. Rel. **8**, 332–343 (2008).
[15] J. A. del Alamo and J. Joh, Microelectron. Reliab. **49**, 1200–1206 (2009).
[16] B. M. Green, K. K. Chu, E. M. Chumbes, J. A. Smart, J. R. Shealy, and L. F. Eastman, IEEE Electron Device Lett. **21**, 268–270 (2000).
[17] Y. Cai, Y. Zhou, K. J. Chen, and K. M. Lau, IEEE Electron Device Lett. **26**, 435–437 (2005).
[18] K. Kobayashi, S. Hatakeyama, T. Yoshida, D. Piedra, T. Palacios, Taiichi Otsuji, and T. Suemitsu, Solid-State Electron. **101**, 63–69 (2014).
[19] S. L. Selvaraj, T. Suzue, and T. Egawa, IEEE Electron Device Lett. **30**, 587–589 (2009).

